### Title
Nature and topology of the low-energy states in ZrTe5




### Journal
Physical Review B, 94(8)

### ISSN
2469-9950



### Authors
Moreschini, L
Johannsen, JC
Berger, H
et al.



### Publication Date
2016-08-01

### DOI
10.1103/physrevb.94.081101

Peer reviewed

PHYSICAL REVIEW B **94**, 081101(R) (2016)

# Nature and topology of the low-energy states in $ZrTe_5$

L. Moreschini,[1,2,3,*] J. C. Johannsen,[1,4] H. Berger,[4] J. Denlinger,[1] C. Jozwiak,[1] E. Rotenberg,[1] K. S. Kim,[2,3] A. Bostwick,[1] and M. Grioni[4]

[1]*Advanced Light Source (ALS), Lawrence Berkeley National Laboratory, Berkeley, California 94720, USA*

[2]*Department of Physics, Pohang University of Science and Technology, Pohang 790-784, Korea*

[3]*Center for Artificial Low Dimensional Electronic Systems, Institute for Basic Science, Pohang 790-784, Korea*

[4]*Institute of Condensed Matter Physics (ICMP), Ecole Polytechnique Fédérale de Lausanne (EPFL), CH-1015 Lausanne, Switzerland*

(Received 19 April 2016; published 4 August 2016; corrected 27 September 2016)

Long known for its peculiar resistivity, showing a thus far unexplained anomalous peak as a function of temperature, $ZrTe_5$ has recently received rising attention in a somewhat different context. While both theoretical and experimental results seem to point to a nontrivial topology of the low-energy electronic states, there is no agreement on the nature of their topological character. Here, by an angle-resolved photoemission study of the evolution of the band structure with temperature and surface doping, we show that (i) the material presents a van Hove singularity close to the Fermi level, and (ii) no surface states exist at the (010) surface. These findings reconcile band structure measurements with transport results and establish the topology of this puzzling compound.

DOI: 10.1103/PhysRevB.94.081101

The first research examples on zirconium pentatelluride $ZrTe_5$ date from the beginning of the 1980s. In those initial studies the source of interest was a peculiar behavior of the electronic transport with temperature. At low temperature the resistivity follows a metallic curve, but it peaks at $T^* \simeq 150$ K and acquires a semiconducting response. At higher temperatures it assumes a slightly positive dependence, reminiscent of a (very poor) metal [1–3]. Lacking evidence for structural or electronic reconstructions [4], such as a charge density wave, there is at present no explanation for these observations. Transport data are complemented by thermoelectric measurements, which attribute negative sign to the charge carriers at $T < T^*$ and positive sign above $T^*$ [5,6]. Shubnikov–de Haas experiments at $T \ll T^*$ yield conflicting results. In one case three Fermi level crossings were found, assigned to one hole (largest) and two electron (medium and smallest) pockets [7]. This would guarantee a semimetal with charge compensation, called for by the even number of $p$ electrons in Te. Another group finds a single Fermi surface [8], and therefore no possible compensation. Theoretical calculations support a semimetallic state at low temperature, with the low-energy bands centered at the $\Gamma$-$Z$ line of the Brillouin zone (BZ) [9,10].

Much more recently, with the rise of topological insulators (TIs), an intense activity on $ZrTe_5$ resumed from a different perspective. Magnetotransport measurements [11,12] and optics [13] appear to be consistent with the presence of three-dimensional (3D) Dirac fermions, which would set this material within the novel class of 3D Dirac semimetals [14,15]. Theory favors instead a gapped electronic structure with band inversion, which translates in single-layer $ZrTe_5$ being (ideally) a two-dimensional (2D) TI and bulk $ZrTe_5$ being at the phase boundary between a strong and a weak TI. The interlayer spacing is believed to play a key role in defining the topological character of the bulk material [16,17].

The few angle-resolved photoemission (ARPES) investigations available to this point [6,11,18–20] agree on the general band mapping of the material, but diverge very evidently in their descriptions of the low-energy states. This Rapid Communication focuses on the low-energy electronic structure and its modifications upon temperature and surface doping, pointing out relevant elements which have been overlooked and providing experimental evidence for the topological classification of $ZrTe_5$ as either a weak TI or a trivial semiconductor.

The crystal structure, shown in Fig. 1(a), consists of chains of Zr atoms embedded in trigonal Te prisms and running along the $a$ axis. The two remaining Te atoms per formula unit bridge two adjacent chains along the $c$ axis. Such pattern forms layers which are then weakly coupled along $b$ by van der Waals forces. The primitive unit cell size is one layer wide in the $b$ direction, and the corresponding reciprocal space is filled with prisms as sketched in Fig. 1(b), elongated along $a^*$ and stacked along $b^*$. It is convenient to use a base-centered orthorhombic cell, shown in Fig. 1(a), which contains instead two layers. The only difference between one layer and the neighboring ones is a translation along $a$ by half the Zr-Zr distance.

The crystals break easily along both the $ab$ and $ac$ planes parallel to the chains, but produce surfaces of measurable size only along $ac$, i.e., at the (010) surface. Throughout this Rapid Communication, in order to maintain the conventional ARPES definition of $k_z$ as oriented normal to the sample surface, we define $x$, $y$, and $z$ as directed along $a$, $c$, and $b$, respectively. The data were collected on the MAESTRO and MERLIN beamlines at the ALS [21].

Figures 1(c)–1(e) show an overview of the band structure measured along the three high-symmetry directions through $\Gamma$ in the $k_x k_y$ plane. The top of the valence band (VB) consists of holelike states yielding the characteristic constant energy contours shown in Fig. 1(g) and already observed in previous work [11]. A preliminary consideration concerns the dimensionality of the material. Whereas structurally it appears clearly one dimensional with needlelike domains, electronically it shows a nearly 2D behavior. The effective

*lmoreschini@lbl.gov

 

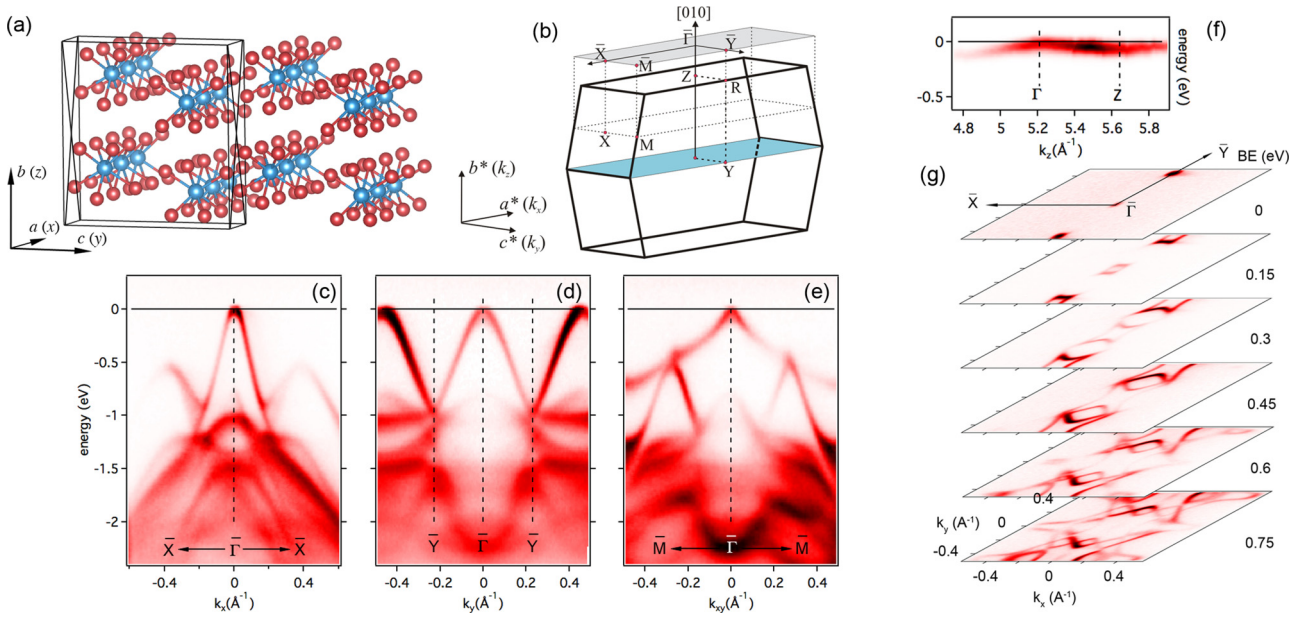


FIG. 1. (a) Real space view of $ZrTe_5$, with Zr and Te atoms in blue and red, respectively, with the conventional unit cell; (b) the 3D BZ with the relevant high-symmetry points. The dark-colored and light-colored planes represent the $k_xk_y$ plane containing $\Gamma$ and the (010) surface BZ, respectively; (c)–(e) band dispersion measured at $h\nu = 69$ eV along the indicated high-symmetry directions; (f) $k_z$ dispersion measured along $\Gamma$-$Z$. $\Gamma$ and $Z$ correspond here to $h\nu = 100$ and 118 eV, respectively. The $k_z$ momentum is evaluated using an inner potential $V_0$ of 7.5 eV; (g) a stack of constant energy cuts taken at the binding energies indicated on the right, for the same dataset of (c)–(e). All the data are measured at $T \simeq 120$ K. The relevant dimensions are $\overline{\Gamma X} = 0.79$ Å$^{-1}$, $\overline{\Gamma Y} = 0.23$ Å$^{-1}$, $\overline{\Gamma M} = 0.82$ Å$^{-1}$, and $\overline{\Gamma Z} = 0.43$ Å$^{-1}$.

mass along $y$ ($\sim -0.09m_e$) is less than twice as large as that along $x$ ($\sim -0.05m_e$), in line with what was observed in transport [22], and much smaller than that along $z$ ($\sim -4.5m_e$). The structural properties are probably determined mostly by the Zr chains, which are well separated along $y$, while electronically the dominant contribution at the top of the VB comes from Te atoms, which form a nearly 2D mesh in the $xy$ plane. Electronically $ZrTe_5$ can thus be treated as a van der Waals layered material.

The bulk sensitivity at the low energies typically used in ARPES is only a few angstrom. Given the large interlayer separation along $z$, $\sim$7.25 Å, it may be questioned whether there is any hope at all to see a signal from electrons below the top atomic layer. As shown in Fig. 1(f), even though the electron escape depth may be small, the wave functions carry information on the periodicity well beyond such escape depth. Photon energy dependent data present indeed a clear oscillation, sign of a moderate (as expected) but measurable $k_z$ dispersion, downwards from $\Gamma$ to $Z$ (holelike).

This was revealed in recent studies [11,19], and used to assign the observed states to the bulk band structure, but another relevant aspect went unnoticed. Figures 2(a) and 2(b) show two close-ups of the band structure measured along $k_x$ for the $\Gamma$ and $Z$ points, respectively. In the former the ARPES intensity engenders a $\Lambda$-shaped dispersion, whereas in the latter the top of the band is clearly M shaped. This point has, as we shall see, profound consequences for the physics of this material.

A closer inspection of Fig. 2(a) reveals a weaker intensity inside the main parabola. This second state is a backfolded replica of the M-shaped band in $Z$. The $ZrTe_5$ structure is known to be prone to slight distortions [23], and it is entirely possible that these could be enhanced close to the surface. In x-ray diffraction data a (1/2,1/2,0) superlattice in the $ab$ plane was observed, which would fold the electronic states into a reduced BZ, only $2\pi/b$ wide in the $k_z$ direction [3,24]. This is seen more clearly in a higher resolution and higher statistics version of Fig. 1(f), shown in Fig. 2(c). The weaker state intensity is completely suppressed in the right half of the figure, but can be nicely followed between $\Gamma$ and half way to $Z$. Note that, given the very slight amount of distortion, attempts to identify two states as a sign of a bilayer splitting do not seem justified, since the lattice primitive cell contains one single layer.

Although clearly the physics of this material is strongly influenced by temperature, the data appearing so far, with one exception [20], are available at sparse temperatures and clearly a systematic study is called for. Figures 2(d)–2(g) show the $k_y$ dispersion of the VB top for $T \gg T^*$ and $T \ll T^*$. At $\Gamma$, the VB maximum is below $E_F$ at high $T$ and shifts well above at low $T$. At $Z$, where the state has higher binding energy, the intensity peak at 40 K does not quite cross $E_F$ yet, and remains instead slightly below. Hence, at low $T$ the band in $Z$ is occupied, and the one in $\Gamma$ is not. This is confirmed by a stack of energy distribution curves (EDCs) measured at $Z$ for decreasing temperatures, shown in Fig. 2(h). The symbols superimposed indicate the fitted peak positions. Another set of symbols indicates, for the subrange of temperatures where the state can be followed, the peak positions obtained by fitting a similar dataset measured at $\Gamma$. Limited to this range the curve is an exact translated version of the one at $Z$ and the band shift is therefore rigid. We verified the shift to be reversible.

Most of the change appears to occur monotonically between $\sim$100 and $\sim$170 K. While a cross comparison between the

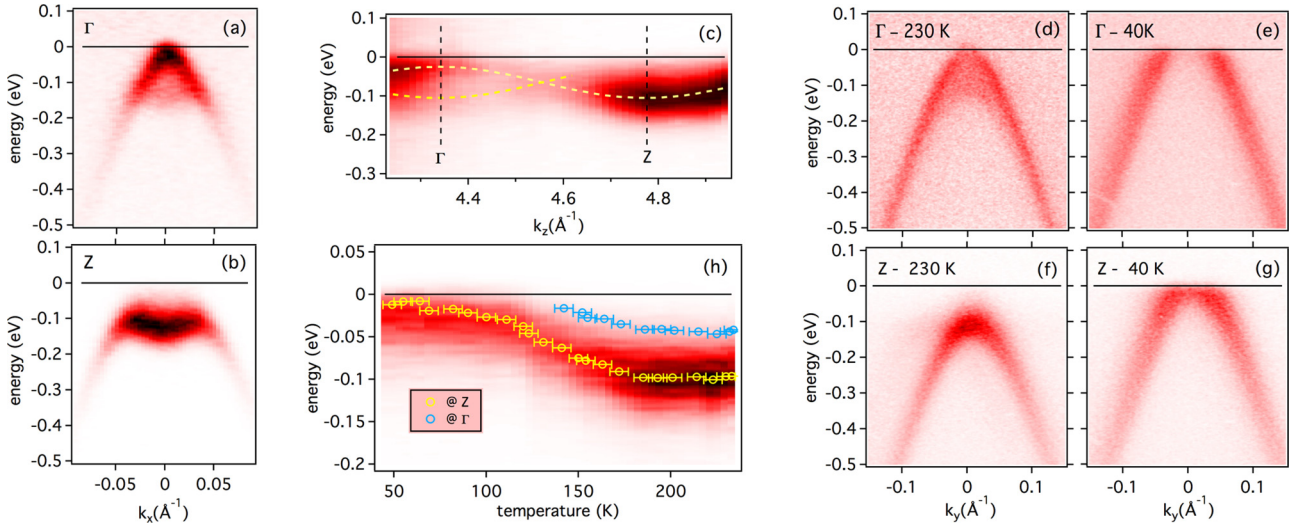


FIG. 2. (a), (b) Valence band dispersion along $k_x$, measured at Γ (69 eV) and $Z$ (83.5 eV), at $T \simeq 160$ K; (c) close-up of the $k_z$ dispersion. The dashed curves are sine waves with period $4\pi/b$, shown as guides to the eye. (d)–(g) valence band dispersion along $k_y$, measured at Γ (69 eV) and $Z$ (83.5 eV) for high and low $T$. Note in (d) the clear backfolded replica of the band in (f); (h) a sequence of EDCs measured at $Z$ for decreasing temperature, shown as an image plot. The yellow symbols indicate the peak positions as obtained by a simple Voigt fit. The blue symbols indicate the peak positions of an equivalent dataset measured for Γ, and limited to the range where the fit is reliable. The intensity of the backfolding is weak and does not flaw the analysis. No normalization has been applied to the data

absolute temperatures may not be wise due to the known influence of defects in the transport properties [3], there exist within previous ARPES data clear contradictions, with some authors observing like us a downward shift of the VB between low and high temperature [19], and others claiming exactly the opposite [6,18,20]. The only other continuous temperature dependence study in a recent preprint shows a monotonous downward shift between room temperature and 2 K [20]. Those data are also peculiar in that the level of electron doping at low $T$ is even larger than obtained by direct surface doping in Ref. [19]. Clearly, extrinsic factors such as the condensation of adsorbates at low temperatures should be carefully considered before attempting a comparison among the existing data, but it seems likely that other elements, such as different defects introduced during the crystal growth, may also play a role in these strong inconsistencies among the different groups.

A key point to notice is that, along $k_y$, both at Γ and $Z$ the VB is holelike [Figs. 2(d) and 2(f)]. It is instead electronlike along $k_x$ at $Z$ [Fig. 2(b)]. Therefore, $Z$ is a saddle point for the band dispersion in the $k_xk_y$ plane, and same in the $k_zk_y$ plane since at $Z$ the dispersion is electronlike in $k_z$ as well. In other words, $ZrTe_5$ presents a 3D van Hove singularity, a possibility hypothesized from optical spectroscopy results [13], with two electronlike axes. Remember that at low $T$ the only occupied states are those close to $Z$. The resulting Fermi surface in 3D is too involved to attempt quantitative electron counting simply from the ARPES data, and furthermore, it is possible that the singularity in the density of states will cause some departures from a rigid band shift in the close proximity of $E_F$ which cannot be fully captured by the experiment. However, the presence of a van Hove singularity with two axes of positive effective mass is central, we believe, for establishing a connection between ARPES results and the transport data at low $T$. Only thanks to the presence of electronlike dispersion along two axes can the Fermi surface consist of electron pockets at low $T$, in agreement with the negative sign of the carriers observed in thermoelectric measurements [5,6].

Note that, while we tried to identify some *consequences* of the observed band shift with temperature, its *origin* remains obscure. Proposals of a strongly asymmetric density of states [19], similarly to the pnictides [25,26], seem unlikely given that the states above and below $E_F$ derive here from the same bands, as opposed to pnictides where electrons and holes are found in two entirely different states. Also, the compensation supposed to hold at all temperatures from the even number of $p$ electrons does not seem consistent with our data, since at higher temperatures only the Λ-shaped state presents a Fermi crossing and no electron pockets can exist. Thus, the description of $ZrTe_5$ as a $p$ semimetal seems too simplistic and some other source of charge has to play a role.

Studying the temperature dependence of the band structure is unfortunately of little help for determining the topological character of $ZrTe_5$. As shown before, the Fermi level moves from slightly above the VB to well within it, so that the conduction band (CB) remains well out of reach. The goal is to discriminate between three proposals appeared thus far: (i) a Dirac semimetal, (ii) a strong TI, and (iii) a weak TI. (i) would result in a bulk Dirac done centered at Γ, with no bulk gap. (ii) is the most common TI case, with a gapped bulk structure and surface states in every crystallographic direction. (iii) would still have surface states, but only on side surfaces, e.g., at step edges, while in the (010) direction it would look just like a standard semiconductor [16].

We could access the CB states by surface doping with alkali atoms, namely, Rb, similar to a recent work where this was achieved by bulk doping using Ta atoms as substitutional defects [19]. In general, if the screening length is not too short, the charge transfer from the alkali is effective in shifting down the bands until the density of the unoccupied states is too large

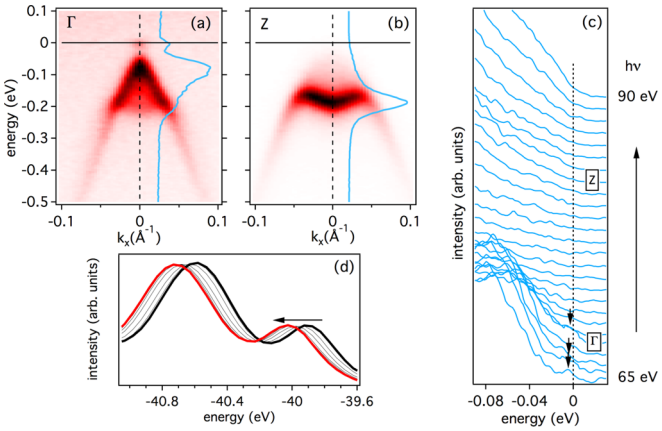


FIG. 3. (a), (b) Equivalents of Figs. 2(a) and 2(b) after deposition of Rb on the sample surface. The spectra superposed to the images are EDCs taken at $k_x = 0$; (c) close-up of a series of (non-normalized) EDCs measured for photon energies of 65–90 eV in steps of 1 eV. The arrows indicate the small intensity at the Fermi level coming from the CB in the vicinity of Γ; (d) evolution of the Te $5d_{5/2}$ core level at successive steps of the Rb deposition. The thick black and red spectra represent the start and end points of the deposition, respectively.

to allow further doping. Figure 3(a) shows the $k_x$ dispersion at Γ after Rb deposition. The EDC in the figure clearly shows a visible tail of the CB at $E_F$, separated by a dip from the VB [27]. This is hard to reconcile with (i) above, since a Dirac semimetal should show no gap.

As further evidence against (i), the energy shift of the Te core levels, shown in Fig. 3(d), after a gradual increase suddenly saturates, as typically observed for semiconductors and insulators [28,29]. The starting point and the amount of the shift are irrelevant and depend on the sample temperature, but the saturation point is always the same, and corresponds roughly to the onset of the CB attaining $E_F$. Assuming a completely symmetric density of states we would deduce a gap of ∼140 meV if extracted as the peak-to-peak energy separation, but the ARPES estimation of the gap in these conditions should be considered a very coarse one.

Even though no Dirac-like dispersion can be seen within the gap, a definite statement is not possible from Fig. 3(a) as the surface state could have a very different intensity from the bulk bands and be nearly completely hidden. Hence we measured [Fig. 3(b)] the $k_x$ dispersion at $Z$, where the (backfolded) Λ-shaped state is extremely weak instead. The EDC extracted at $Z$ is completely flat at $E_F$, with no trace of an additional state. A stack of EDCs over the full Γ-$Z$ range (and beyond) is shown in Fig. 3(c). The statistics is worse than in Figs. 3(a) and 3(b) due to time constraints in measuring the whole range without a sizable desorption of Rb from the surface, but small features at the Fermi level (see arrows) can only be found at the photon energies close to Γ. Elsewhere, the EDCs are featureless close to $E_F$. The presence of a surface state can thus be excluded, and scenario (ii) ruled out.

Our results certainly favor a weak TI as a correct description of $ZrTe_5$, or a standard semiconductor in lack of band inversion. However, since $ZrTe_5$ is supposed to be at the edge between (ii) and (iii) [16,17], we cannot dismiss the possibility that the Rb deposition could modify the interlayer separation enough to shift the material from one side to the other of the phase space. The direct measurement of edge states, predicted for a weak TI and rather convincingly shown by tunneling spectroscopy in recent reports [19,30], will be a stimulating challenge for the existing and upcoming nanoARPES facilities.

We gratefully acknowledge A. Crepaldi and G. Autès for discussing with us their data during the preparation of this Rapid Communication, M. Gherardi for interesting discussions, and Yeongkwan Kim for technical support on MERLIN. The Advanced Light Source is supported by the Director, Office of Science, Office of Basic Energy Sciences, of the US Department of Energy under Contract No. DE-AC02-05CH11231.

[1] S. Okada, T. Sambongi, and M. Ido, J. Phys. Soc. Jpn. **49**, 839 (1980).
[2] E. Skelton, T. Wieting, S. Wolf, W. Fuller, D. Gubser, T. Francavilla, and F. Levy, Solid State Commun. **42**, 1 (1982).
[3] F. J. DiSalvo, R. M. Fleming, and J. V. Waszczak, Phys. Rev. B **24**, 2935 (1981).
[4] S. Okada, T. Sambongi, M. Ido, Y. Tazuke, R. Aoki, and O. Fujita, J. Phys. Soc. Jpn. **51**, 460 (1982).
[5] T. Jones, W. Fuller, T. Wieting, and F. Levy, Solid State Commun. **42**, 793 (1982).
[6] D. N. McIlroy, S. Moore, D. Zhang, J. Wharton, B. Kempton, R. Littleton, M. Wilson, T. M. Tritt, and C. G. Olson, J. Phys.: Condens. Matter **16**, L359 (2004).
[7] G. N. Kamm, D. J. Gillespie, A. C. Ehrlich, T. J. Wieting, and F. Levy, Phys. Rev. B **31**, 7617 (1985).
[8] M. Izumi, T. Nakayama, K. Uchinokura, S. Harada, R. Yoshizaki, and E. Matsuura, J. Phys. C **20**, 3691 (1987).
[9] M. H. Whangbo, F. J. DiSalvo, and R. M. Fleming, Phys. Rev. B **26**, 687 (1982).
[10] D. Bullett, Solid State Commun. **42**, 691 (1982).
[11] Q. Li, D. E. Kharzeev, C. Zhang, Y. Huang, I. Pletikosić, A. V. Fedorov, R. D. Zhong, G. A. Schneeloch, G. D. Gu, and T. Valla, Nat. Phys. **12**, 550 (2016).
[12] R. Y. Chen, Z. G. Chen, X.-Y. Song, J. A. Schneeloch, G. D. Gu, F. Wang, and N. L. Wang, Phys. Rev. Lett. **115**, 176404 (2015).
[13] R. Y. Chen, S. J. Zhang, J. A. Schneeloch, C. Zhang, Q. Li, G. D. Gu, and N. L. Wang, Phys. Rev. B **92**, 075107 (2015).
[14] Z. K. Liu, B. Zhou, Y. Zhang, Z. J. Wang, H. M. Weng, D. Prabhakaran, S.-K. Mo, Z. X. Shen, Z. Fang, X. Dai *et al.*, Science **343**, 864 (2014).
[15] M. Neupane, S.-Y. Xu, R. Sankar, N. Alidoust, G. Bian, C. Liu, I. Belopolski, T.-R. Chang, H.-T. Jeng, H. Lin *et al.*, Nat. Commun. **5**, 3786 (2014).
[16] H. Weng, X. Dai, and Z. Fang, Phys. Rev. X **4**, 011002 (2014).

[17] O. Yazyev and G. Autès (private communication).

[18] G. Manzoni, A. Sterzi, A. Crepaldi, M. Diego, F. Cilento, M. Zacchigna, P. Bugnon, H. Berger, A. Magrez, M. Grioni *et al.*, Phys. Rev. Lett. **115**, 207402 (2015).

[19] R. Wu, J.-Z. Ma, S.-M. Nie, L.-X. Zhao, X. Huang, J.-X. Yin, B.-B. Fu, P. Richard, G.-F. Chen, Z. Fang *et al.*, Phys. Rev. X **6**, 021017 (2016).

[20] Y. Zhang, C. Wang, L. Yu, G. Liu, A. Liang, J. Huang, S. Nie, Y. Zhang, B. Shen, J. Liu *et al.*, arXiv:1602.03576.

[21] See Supplemental Material at http://link.aps.org/supplemental/10.1103/PhysRevB.94.081101 for experimental details and a discussion of the temperature dependence.

[22] The anisotropy in the resistivity was reported to grow from $\sim 2$ up to a $\sim 10$ at low temperatures (Ref. [4]). We tend to believe, though, that these factors also include extrinsic terms due to the structural mismatch between the different domains along $y$, which affect the flow of the charge carriers.

[23] D. J. Eagleshamt, J. Mulcahy, and J. A. Wilson, J. Phys. C **20**, 351 (1987).

[24] J. A. Wilson, Philos. Trans. R. Soc. London **314**, 159 (1985).

[25] R. S. Dhaka, S. E. Hahn, E. Razzoli, R. Jiang, M. Shi, B. N. Harmon, A. Thaler, S. L. Bud'ko, P. C. Canfield, and A. Kaminski, Phys. Rev. Lett. **110**, 067002 (2013).

[26] V. Brouet, P.-H. Lin, Y. Texier, J. Bobroff, A. Taleb-Ibrahimi, P. Le Fèvre, F. Bertran, M. Casula, P. Werner, S. Biermann *et al.*, Phys. Rev. Lett. **110**, 167002 (2013).

[27] The sample was aligned within $0.05^\circ$ because, with the CB minimum so close to the Fermi level, an apparent gap could be easily produced even by a very slight misalignment.

[28] L. Moreschini, G. Autès, A. Crepaldi, S. Moser, J. Johannsen, K. Kim, H. Berger, P. Bugnon, A. Magrez, J. Denlinger *et al.*, J. Electron Spectrosc. Relat. Phenom. **201**, 115 (2015).

[29] R. Comin, G. Levy, B. Ludbrook, Z.-H. Zhu, C. N. Veenstra, J. A. Rosen, Y. Singh, P. Gegenwart, D. Stricker, J. N. Hancock *et al.*, Phys. Rev. Lett. **109**, 266406 (2012).

[30] X.-B. Li, W.-K. Huang, Y.-Y. Lv, K.-W. Zhang, C.-L. Yang, B.-B. Zhang, Y. B. Chen, S.-H. Yao, J. Zhou, M.-H. Lu *et al.*, Phys. Rev. Lett. **116**, 176803 (2016).

# Supplemental Material:

# Nature and topology of the low energy states in $ZrTe_5$

L. Moreschini,[1,2,3] J. C. Johannsen,[1,4] H. Berger,[4] J. Denlinger,[1] C. Jozwiack,[1] E. Rotenberg,[1] K. S. Kim,[2,3] A. Bostwick,[1] and M. Grioni[4]

[1]*Advanced Light Source (ALS), Lawrence Berkeley National Laboratory, Berkeley, California 94720, USA*

[2]*Departement of Physics, Pohang University of Science and Technology, Pohang 790-784, Korea*

[3]*Center for Artificial Low Dimensional Electronic Systems, Institute for Basic Science, Pohang 790-784, Korea*

[4]*Institute of Condensed Matter Physics (ICMP), Ecole Polytechnique Fédérale de Lausanne (EPFL), CH-1015 Lausanne, Switzerland*

## EXPERIMENTAL DETAILS

The ARPES experiments were performed both at the MAESTRO and MERLIN beamlines of the Advanced Light Source in Berkeley. The energy and momentum resolution were ∼15 meV and 0.1°. The experimental geometry for the two endstations is sketched in Fig. S1. Both beamlines are equipped with vertical and horizontal polarization, but here we used only $p$ (horizontally) polarized light. since the synchrotron beam is smaller in the vertical direction than in the horizontal one, in order to avoid multiple domains it is more convenient to orient the $a$ (needle-like) direction of the crystal horizontally. Therefore MAESTRO was mostly used to measure along the Γ-X direction [figs. 1, 2(a-c) and 3], while MERLIN was used for the maps along Γ-Y [fig. 2(d-h)]. The photon energy dependence was confirmed on both beamlines.

The Fermi level was measured either on a piece of gold foil in contact with the sample holder, or on the copper sample holder itself, scraped in vacuum. We estimate the uncertainty to be less than 10 meV. Rb was deposited on the surface by a getter commercial evaporator in successive steps of 35 seconds. After each step a quick dataset was acquired until the tail of the conduction band became visible. Further Rb deposition does not cause a further shift of the bands, but rather a worsening of the surface quality.

Single crystals of $ZrTe_5$ were grown from high purity elements Zr (99.9%, metal basis excluding 2.5% Hf) and Te (99.999%) by chemical transport using iodine as the transport agent. The mixture was sealed in a quartz tube under vacuum, placed horizontally into a tubular two-zone furnace and heated very slowly with a rate of 50°C/h to 530°C. For the growth of single crystals, the optimum temperatures at the source and deposition zones have been established as 530°C and

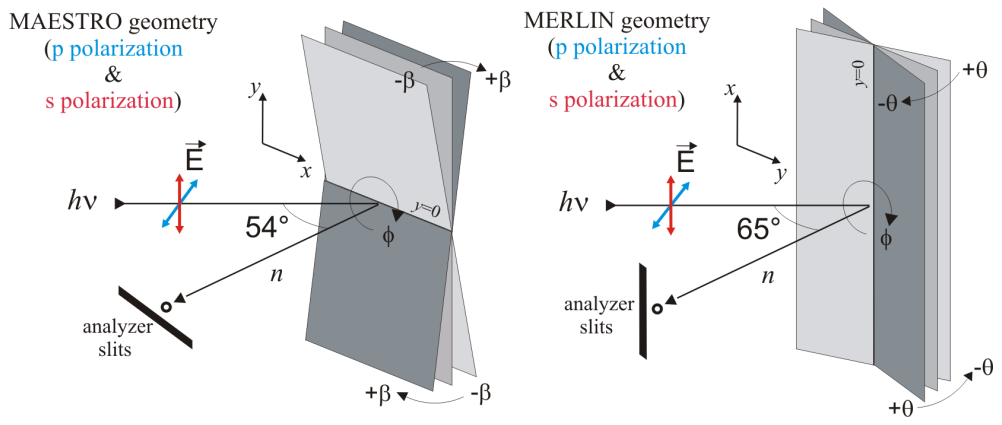


FIG. S1: Experimental geometry of the two beamlines used for the measurements in this study

480°C, respectively. After about 3 to 5 weeks, crystals with a maximum size of $\sim 1 \times 1 \times 25$ mm$^3$ are obtained. The longest direction is always along the crystallographic $a$ axis. The composition was determined by single-crystal X-ray diffraction. More details are available in Ref. 1.

## A QUICK OVERVIEW OF THE TEMPERATURE DEPENDENCE SHOWN IN PREVIOUS ARPES STUDIES

Although more recently $ZrTe_5$ has received much attention as a possible topologically non trivial material, the different groups have attempted to find a logical explanation to the older puzzle of the anomalous transport properties. The resistivity of $ZrTe_5$ mimics that of a semiconductor at high temperatures and that of a metal at low temperatures, with a broad maximum in between at $\sim$150K, very sample dependent. The charge carriers change sign between the two regimes, from holes at high T to electrons at low T. In chronological order:

- Ref. 2 shows data at two discrete temperatures, 170K and 75K, with a downward shift of the valence band by $\sim$40 meV from intermediate to low T.
- Ref. 3 shows data at two discrete temperatures, 300K and 125K, with a downward shift of the valence band by $\sim$60 meV from high to intermediate T.
- Ref. 4 shows data at two discrete temperatures, 200K and 25K, with an upward shift of the valence band by $\sim$30 meV from high to low T (value extracted from the figure, not explicitly declared in the text).
- Ref. 5 shows data at two discrete temperatures, 200K and 24K, with an upward shift of the valence band by $\sim$60 meV from high to low T (value extracted from the figure, not explicitly declared in the text).
- Ref. 6 shows several data points from 255K to 2K, with a total downward shift of the valence band by $\sim$70 meV from high to low T and a shift of the Fermi level well into the conduction band for low temperatures.

In the main text, we show a continuous temperature evolution from 250K to 40K, with a total upward shift of the valence band by $\sim$100 meV from high to low T, occurring mainly between 170K and 100K. Clearly, our data are more consistent with refs. 4 and 5, whereas refs. 2, 3 and 6 show an opposite trend. The only plausible origins for the differences observed are

different sample defects or different measurement conditions (adsorbants in the UHV chamber). Note that defects are known to play a role in this compound already from the strong variations in the resistivity peak temperature between the different groups in old studies. A possible influence of the surface termination does not seem to be an option here, since there is only one likely cleaving plane along the $b$ axis of the crystal.

One issue is to explain the reason of the temperature shift of the Fermi level. A separate one is to reconcile the observed band structure with the transport data.

On the former point, in lack of evidence of any structural or electronic transition, some authors hypothesize a very asymmetric density of states [5], similarly to the pnictides, while others point to a role of the gradual thermal variations of the lattice parameters [6, 7]. This second possibility could be an interesting playground for theorists, given the available diffraction data as a function of temperature [8].

On the latter point, the sign of the shift leads to two different scenarios. Groups observing a downward shift of the bands decreasing the temperature see a p-type metal at room temperature, a p-type semiconductor at intermediate temperatures, and an n-type metal at low temperature. The switch of the carriers sign is caused by the Fermi level moving from the valence band to the conduction band [2, 3, 6]. Groups seeing an upward shift see a p-type semiconductor at high temperature and an n-type metal at low temperature [4, 5]. As we show here the switch of the carrier sign is due instead to the Fermi level moving from the valence band maximum at the $\Gamma$ point to the van Hove singularity at the Z point. Since the van Hove singularity has two electron-like axes at Z, the carriers have negative sign.

Without further elements, it is difficult to rule out one of the two interpretations. It is worthwhile to note that both scenarios cannot be explained within a regime of charge compensation and require some charges to undergo localization/delocalization as a function of T. It seems clear therefore that the behavior of an ideal defect-free $ZrTe_5$ would show qualitative differences with what reported so far.

[1] F. Levy and H. Berger, Journal of Crystal Growth **61**, 61 (1983).

[2] D. N. McIlroy, S. Moore, D. Zhang, J. Wharton, B. Kempton, et al., Journal of Physics: Condensed Matter **16**, L359 (2004).

[3] G. Manzoni, A. Sterzi, A. Crepaldi, M. Diego, F. Cilento, et al., Phys. Rev. Lett. **115**, 207402 (2015).

[4] Q. Li, D. E. Kharzeev, C. Zhang, Y. Huang, I. Pletikosić, et al. (2014), arXiv:1412.6543.

[5] R. Wu, J.-Z. Ma, S.-M. Nie, L.-X. Zhao, X. Huang, et al., Phys. Rev. X **6**, 021017 (2016).

[6] Y. Zhang, C. Wang, L. Yu, G. Liu, A. Liang, et al. (2016), arXiv:1602.03576.

[7] R. Y. Chen, S. J. Zhang, J. A. Schneeloch, C. Zhang, Q. Li, et al., Phys. Rev. B **92**, 075107 (2015).

[8] H. Fjellvag and A. Kjekshus, Solid State Communications **60**, 91 (1986).